



LAWRENCE  
LIVERMORE  
NATIONAL  
LABORATORY

# Direct-Semidirect Thermal Neutron Capture Calculations

G. Arbanas, F. S. Dietrich, A. K. Kerman

December 21, 2005

Perspectives on Nuclear Data for the Next Decade  
Bruyeres-le-Chatel, France  
September 26, 2005 through September 28, 2005

## **Disclaimer**

---

This document was prepared as an account of work sponsored by an agency of the United States Government. Neither the United States Government nor the University of California nor any of their employees, makes any warranty, express or implied, or assumes any legal liability or responsibility for the accuracy, completeness, or usefulness of any information, apparatus, product, or process disclosed, or represents that its use would not infringe privately owned rights. Reference herein to any specific commercial product, process, or service by trade name, trademark, manufacturer, or otherwise, does not necessarily constitute or imply its endorsement, recommendation, or favoring by the United States Government or the University of California. The views and opinions of authors expressed herein do not necessarily state or reflect those of the United States Government or the University of California, and shall not be used for advertising or product endorsement purposes.

# Direct-Semidirect Thermal Neutron Capture Calculations

G. Arbanas  
Oak Ridge National Laboratory  
Oak Ridge, TN 37831, U.S.A.

F. S. Dietrich  
Lawrence Livermore National Laboratory  
Livermore, CA 94550, U.S.A.

A. K. Kerman  
Massachusetts Institute of Technology  
Cambridge, MA 02139, U.S.A.

## Abstract

A method for computing direct-semidirect (DSD) neutron radiative capture is presented and applied to thermal neutron capture on  $^{19}\text{F}$ ,  $^{27}\text{Al}$ ,  $^{28,29,30}\text{Si}$ ,  $^{35,37}\text{Cl}$ ,  $^{39,41}\text{K}$ ,  $^{56}\text{Fe}$ , and  $^{238}\text{U}$ , in support of data evaluation effort at the O.R.N.L. The DSD method includes both direct and semidirect capture; the latter is a core-polarization term in which the giant dipole resonance is formed.

We study the effects of a commonly used “density” approximation to the EM operator and find it to be unsatisfactory for the nuclei considered here. We also study the magnitude of semidirect capture relative to the pure direct capture. Furthermore, we compare our results with those obtained from another direct capture code (TEDCA [17]). We also compare our results with those obtained from analytical expression for external capture derived by Lane and Lynn [3], and its extension to include internal capture [7].

To estimate the effect of nuclear deformation on direct capture, we computed direct thermal capture on  $^{238}\text{U}$  with and without imposition of spherical symmetry. Direct capture for a spherically symmetric  $^{238}\text{U}$  was approximately 6 mb, while a quadrupole deformation of 0.215 on the shape of  $^{238}\text{U}$  lowers this cross section down to approximately 2 mb. This result suggests that effects of nuclear deformation on direct capture warrant a further study. We also find out that contribution to the direct capture on  $^{238}\text{U}$  from the nuclear interior significantly cancels that coming from the exterior region, and hence both contributions must be taken into account.

We reproduced a well known discrepancy between the computed and observed branching ratios in  $^{56}\text{Fe}(n, \gamma)$ . This will lead us to revisit the concept of doorway states in the particle-hole model.

# 1 Introduction

For nuclear data evaluations in the resolved resonance region direct capture may be significant between resonant capture peaks, as well as at very low neutron incident energy below the lowest resonance (e.g. thermal capture). Experimental data is subject to background effects that, at energies below 10 keV, could be sufficiently large to obscure the direct capture cross section. This has motivated the theoretical calculations of direct capture cross section presented here.

Since the density form of the EM operator is commonly used in computations of direct capture, we investigated the validity of this approximation by comparing direct capture cross sections computed with and without this approximation, which results from applying Siegert's theorem to the more complete current form of the operator. Lafferty and Cotanch [1] have studied the application of the density approximation, warning that its effect could be very large.

The study of the effects of the semidirect term of the EM operator was inspired by similar studies of direct-semidirect capture near and above the GDR energy, that is 10-20 MeV, where the semidirect term is essential for explaining the experimental data ([4], [5], and [6]).

# 2 Radiative Capture Formalism

A rather complete description of the formulae for calculating direct-semidirect capture was given in Appendix A of Parker *et al.* [2]. The expressions in that paper were embodied in the CUPIDO program. For the present application we are interested principally in capture to separate bound states, and the formulas simplify considerably. We show here a reduction of formula (A1) of Ref. [2] for this case, and also specialize to electric radiation described by the density form of the electromagnetic operator in the long-wavelength limit.

We adopt the notation in Ref. [2] in the following, and refer the reader to that article for definitions of most of the symbols. The expressions below are for capture of spin- $\frac{1}{2}$  nucleons on a spin-0 target into a pure single-particle orbital characterized by quantum numbers  $n_f l_f j_f$ .

For direct capture a radial electric operator in a density approximation has the following form:

$$O_L = e_{\text{eff}} r^L. \tag{1}$$

The symbol  $e_{\text{eff}}$  stands for kinematic effective charge defined by Eq. (A17) of Ref. [2] as

$$e_{\text{eff}} = (-1)^L Z \left( \frac{1}{A+1} \right)^L + z \left( \frac{A}{A+1} \right)^L, \tag{2}$$

in which  $Z, A$  are the charge and mass number of the target, and  $z$  is the charge of the projectile. We also define radial matrix elements

$$\mathcal{I}_c^{n_f l_f j_f} = \int_0^\infty dr u_{n_f l_f j_f} O_L u_{l_j}^{(+)}, \tag{3}$$

$$\mathcal{J}_c^{n_f l_f j_f} = \int_0^\infty dr u_{n_f l_f j_f} O_{L-1} \frac{d}{dr} u_{l_j}^{(+)}, \tag{4}$$

$$\mathcal{K}_c^{n_f l_f j_f} = \int_0^\infty dr u_{n_f l_f j_f} O_{L-2} u_{l_j}^{(+)}. \tag{5}$$

For the density form of the electromagnetic operator, we calculate the amplitudes for direct capture in each channel  $c \equiv \{ljL\sigma\}$  as

$$\mathcal{G}_c^{n_f l_f j_f} = k_\gamma^L i^{-l-l_f+L} e^{i\sigma_l} \frac{1}{(2L+1)!!} \sqrt{\frac{L+1}{L}} \frac{1}{\sqrt{2j+1}} \bar{Z}(l_f j_f l j; \frac{1}{2}L) \mathcal{I}_c^{n_f l_f j_f}. \quad (6)$$

For the current form of the operator for direct capture, the amplitudes are

$$\begin{aligned} \mathcal{G}_c^{n_f l_f j_f} &= (-1)^{j+j_f} \frac{\hbar c}{\mu c^2} k_\gamma^{L-1} i^{l-l_f-L} e^{i\sigma_l} \frac{1}{(2L+1)!!} \sqrt{\frac{(L+1)(2L+1)(2j_f+1)}{2l+1}} \\ &\times \left\{ \begin{array}{ccc} l_f & j_f & \frac{1}{2} \\ j & l & L \end{array} \right\} \left\{ \sqrt{l+1} \bar{Z}(l+1, l, L-1, L; 1, l_f) \left[ \mathcal{J}_c^{n_f l_f j_f} - (l+1) \mathcal{K}_c^{n_f l_f j_f} \right] \right. \\ &\quad \left. - \sqrt{l} \bar{Z}(l-1, l, L-1, L; 1, l_f) \left[ \mathcal{J}_c^{n_f l_f j_f} + l \mathcal{K}_c^{n_f l_f j_f} \right] \right\}. \quad (7) \end{aligned}$$

Direct capture amplitudes are supplemented by semidirect amplitudes using a semidirect transition operator:

$$O_L^{DSD} = \sum_T h'_{LT}(r) \left( \frac{1}{E_\gamma - E_{LT} + i\Gamma_{LT}/2} - \frac{1}{E_\gamma + E_{LT}} \right) \quad (8)$$

where the  $E_{LT}$  and  $\Gamma_{LT}$  are the position and the width of the giant resonance of multipolarity and isospin  $L, T$ , and  $h'_{LT}(r)$  is a form factor described in more detail in Eqs. (A23-A25) of Parker et al. [2] and references therein.

For our purposes here we only need the total (angle-integrated) cross section, which can be expressed in terms of the above quantities as:

$$\sigma_\gamma^{n_f l_f j_f} = 4\pi\alpha \frac{\mu c^2}{\hbar c} \frac{k_\gamma}{k_i^3} \sum_c (2j+1) \left| \mathcal{G}_c^{n_f l_f j_f} \right|^2. \quad (9)$$

For simplicity, we will drop the subscript from the quantum numbers ( $n_f l_f j_f$ ) as there is no longer an ambiguity.

The total radiative capture cross sections is the sum of of capture cross sections into all available orbitals  $nlj$

$$\sigma_\gamma^{actual} = \sum_{nlj} \frac{2J_f + 1}{2J_i + 1} \frac{S_{nlj}}{2j + 1} \sigma_\gamma^{nlj}. \quad (10)$$

The quantity in the sum in front of the calculated cross section is the weight factor  $W$ .  $\gamma$ -branching ratios are determined by comparing relative contributions of capture to individual ( $n, l, j$ ) bound states to their sum.

### 3 Results

Our results for direct-semidirect capture on  $^{19}\text{F}$ ,  $^{27}\text{Al}$ ,  $^{28,29,30}\text{Si}$ ,  $^{35,37}\text{Cl}$ , and  $^{39,41}\text{K}$  are summarized in Table 1. We observe a very good agreement with the theoretical results of Raman-Lynn on  $^{19}\text{F}$  [15] and  $^{28,29,30}\text{Si}$  [14], where the gamma-branching ratios for both computations are in close agreement with the experiment.

All of our results presented in this work were obtained using a real part of the global Koning-Delaroche OMP [11] for the scattering states, and a Bear-Hodgson [12] potential for the bound states. The depth of the Bear-Hodgson potential was adjusted to give the known binding energy of the capturing levels.

Author	$^{19}\text{F}$	$^{27}\text{Al}$	$^{28}\text{Si}$	$^{29}\text{Si}$	$^{30}\text{Si}$	$^{35}\text{Cl}$	$^{37}\text{Cl}$	$^{39}\text{K}$	$^{41}\text{K}$
This work	6.5	60	133	111	98	430	418	799	544
TEDCA [18] [19]	—	—	65	58	67	160	310	—	—
Raman-Lynn	4.6	—	134	116	100	—	—	—	—
Lane-Lynn	4.7	108	107	70	64	—	400	753	1,320
Exp.	9.5	231	169	119	107	43,600	433	2,100	1,460

Table 1: Summary of thermal capture results and comparison with prior works; all cross sections are stated in mb; a systematic error of  $\pm 20\%$  comes mostly from the uncertainty in the measurements of the spectroscopic factors

EM operator	$^{19}\text{F}$	$^{27}\text{Al}$	$^{28}\text{Si}$	$^{29}\text{Si}$	$^{30}\text{Si}$	$^{35}\text{Cl}$	$^{37}\text{Cl}$	$^{39}\text{K}$	$^{41}\text{K}$
Current	6.5	60	133	111	98	430	418	799	544
Density	2.7	42	108	90	83	408	411	839	577
Exp.	9.5	231	169	119	107	43,600	433	2,100	1,460

Table 2: Comparison of DSD when using a current vs. density form of the EM operator; the real part of the global Koning-Delaroche OMP [11] was used for the scattering states, Bear-Hodgson potential for the bound states.

As a side note, we took advantage of available measurements of thermal capture  $\gamma$ -branching ratios for the nuclei under study here, for comparison with  $\gamma$ -branching ratios obtained from our computation of DSD capture. For nuclides for which direct capture is a dominant mechanism, such as  $^{28,29,30}\text{Si}$  and  $^{37}\text{Cl}$ , the agreement between the experimental and computed  $\gamma$ -rays branching ratios is very close. On the other hand, for  $^{35}\text{Cl}$  there is no correlation between the experimental and computed branching ratios as the thermal capture is dominated by a nearby resonance. A similar lack of correlation has been observed in  $^{39,41}\text{K}$  where non-direct capture dominates, albeit not as one-sidedly as in the case of  $^{35}\text{Cl}$ . We observed some correlation between the experimental and DSD capture branching ratios in  $^{19}\text{F}$  and  $^{27}\text{Al}$  even though there is a large contribution from the non-direct, i.e. compound capture.

### 3.1 Current vs. Density EM Operator on $sd$ -shell Nuclei

Table 2. summarizes the DSD capture results obtained with (exact) current form of the EM operator vs. their equivalents obtained with the density form approximation. The current form gives a result that is a factor of two larger than a corresponding approximate density form for capture on  $^{19}\text{F}$ . The discrepancy decreases with increasing target mass, as can be seen in Table 2. Considering the magnitude of this discrepancy we would like to recommend usage of the current form of the operator. Formal aspects of current vs. density form of EM operator were discussed on page 259 of Parker *et al.* [2].

### 3.2 Direct vs. DSD capture on $sd$ -shell Nuclei

The effect of semidirect capture was found to be approximately 5% of the DSD thermal capture cross section. This effect can, however, reach  $\sim 30\%$  for low energy  $p$ -wave  $E1$  transitions, and hence could be important for those nuclide that do not have large spectroscopic factors for  $l = 1$  bound states that are needed for low energy  $E1$  capture of  $s$ -wave neutrons. Note that the effect of semidirect can be positive or negative, depending on the nature of interference between direct and semidirect capture amplitudes.

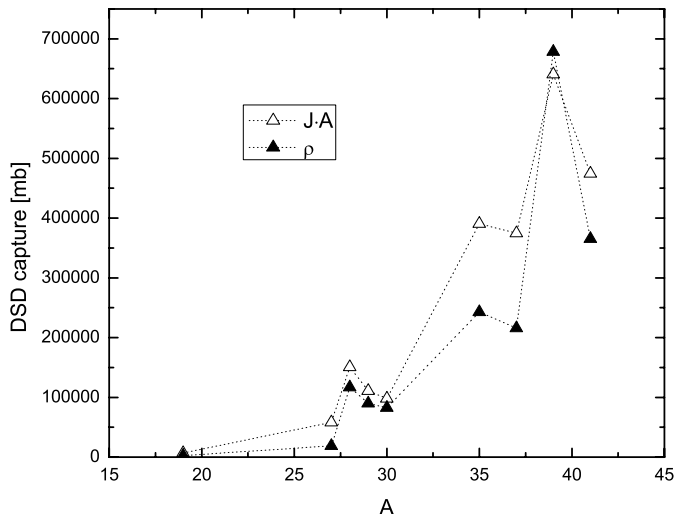


Figure 1: Thermal neutron capture cross section computed with the (exact) current form vs. density form of the EM operator suggests that density form of the EM operator is not a good approximation. (It turns out that semidirect capture does not significantly affect the plotted *thermal* capture on *sd* shell nuclei, so we do not plot it for the sake of clarity.)

### 3.3 Direct Capture on $^{238}\text{U}$

We computed pure direct capture of thermal neutrons on  $^{238}\text{U}$  in order to study effects of nuclear shape deformation on computation of direct capture. We also sought to find relative contributions to direct capture from inside and outside the nuclear volume. For simplicity we did not include semidirect capture in this computation.

We found that  $^{238}\text{U}$  quadrupole deformation of  $\beta = 0.215$  cuts the direct capture cross section from 6 mb (obtained by imposing spherical symmetry) down to 2 mb [16]. To account for the effects of non-spherical nuclear shape, we employed a coupled-channels reactions code FRESKO ([20]) and compared the results with those obtained by CUPIDO in which a spherical symmetry is imposed.

We studied relative contribution of the internal vs. external capture by plotting the amplitude of the dominant E1 transition as a function of radius. We observed that the amplitude for the interior capture is comparable but opposite in sign to the external capture, so that significant cancellation occurs when performing radial integration of the plotted amplitude. This observation explains for the most part the large discrepancy between 60 mb obtained in [13] by taking into account only external capture, and our direct capture computation of 6 mb. Both of these results were obtained in a spherically symmetric approximation.

### 3.4 DSD Capture on $^{56}\text{Fe}$

Our interest in  $^{56}\text{Fe}(n,\gamma)$  for thermal neutrons was sparked by the known discrepancy between the computed and observed  $\gamma$ -branching ratios. It has been hypothesized that this discrepancy may be explained by the  $3s$  doorway state that is expected to be near zero energy for the  $A \approx 60$  nuclei. This hypothesis motivated our interest in capture through doorway states of particle-hole character. Such

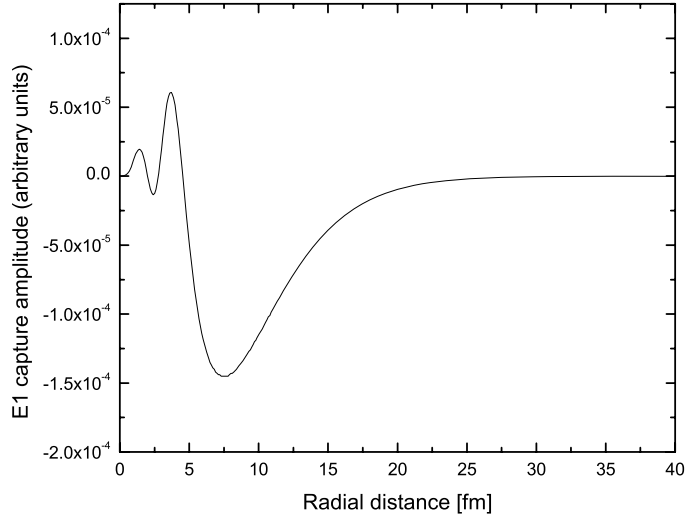


Figure 2: Integrand of the thermal neutron direct capture amplitude for the dominant E1 transition to  $E_x = 4.935$  MeV  $2p_{3/2}$  level in  $^{28}\text{Si}$  shows that the contribution of the external (namely  $r > 4$  fm) capture is much larger than the internal contribution, and hence approximating the capture by its external part alone, as was done by Lane & Lynn in [3], is a good approximation for this nucleus.

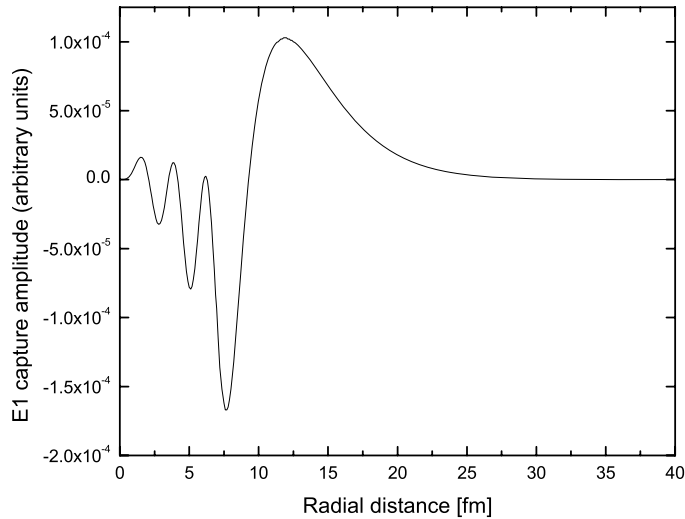


Figure 3: Integrand of the thermal neutron direct capture amplitude for the dominant E1 transition to  $E_x = 746$  keV  $3p_{1/2}$  level in  $^{238}\text{U}$  shows that internal (namely  $r < 8.4$  fm) capture is comparable to the external capture but of opposite sign, and hence the pure external capture of Lane-Lynn [3] is not a good approximation for heavy nuclei.

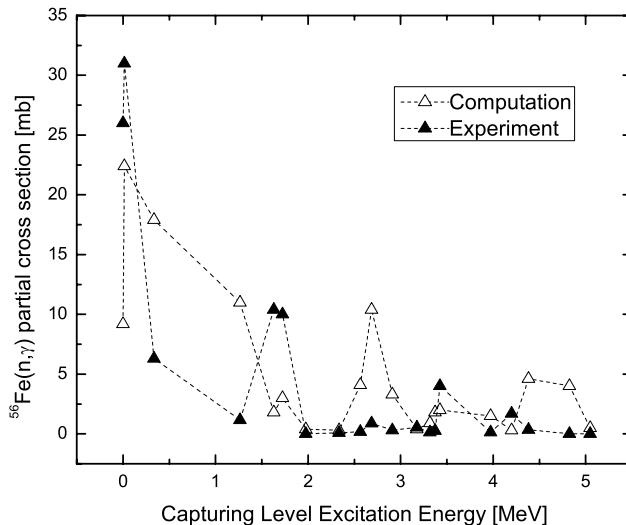


Figure 4: Thermal neutron capture cross sections to individual excited states in  $^{56}\text{Fe}$  show a large discrepancy between the computation and experiment. This may indicate that the spectroscopic factors obtained from  $^{56}\text{Fe}(d,n)$  experiments do not explain observed distribution of  $\gamma$ -rays in  $(n,\gamma)$  experiment. This discrepancy may be explained by the concept of doorway states, as was suggested in [9] and [8]

doorway states may be obtained from the Gamow shell model [10], since this shell model is capable of computing particle-hole components of excited levels, including those in the continuum.

## 4 Conclusions and Outlook

We presented a set of DSD capture computations at thermal energy for several *sd* shell nuclei, and find an agreement within the error margins with the results obtained by Lane-Lynn prescription [13] and by Raman's collaboration (e.g. [14] and [15]). Comparison to the results obtained by TEDCA reveals that TEDCA results are smaller than ours, in part due to the density approximation to the EM operator that is implemented in TEDCA.

Our results indicate that in many cases the DSD capture cross section obtained with exact current form of the EM operator could be quite different than its equivalent obtained with the approximate density form. Consequently we recommend using the exact current form of the EM operator. We also recommend including the semidirect capture together with the direct one, as it can affect p-wave capture even at energies as low as thermal. Both of these effects need to be studied at higher energies in the resolved resonance region.

The large effect of nuclear shape deformation on direct capture on  $^{238}\text{U}$  warrants further study of such effects.

We reproduced a well known discrepancy between the computed and observed branching ratios in  $^{56}\text{Fe}(n,\gamma)$ . This will lead us to revisit the concept of doorway states (Feshbach, Kerman, and Lemmer [8]) and to consider its application to direct capture, as has already been done in qualitative terms by Ikegami, and Emery [9].

## 5 Acknowledgments

We thank Prof. Ian Thompson for a computation of direct capture of thermal neutrons on spherically deformed  $^{238}\text{U}$ , allowing us to quantify the effect of nuclear deformation on direct capture.

This work was performed under the auspices of the U.S. Department of Energy by DE-AC05-00OR22725 and by the University of California, Lawrence Livermore National Laboratory under contract No. W-7405-Eng-48.

## References

- [1] J. M. Lafferty, and S. R. Cotanch, Nucl. Phys. **A373**, 363 (1982)
- [2] W. E. Parker *et al.*, Phys. Rev. C **52**, 252 (1995)
- [3] A. M. Lane, and J. E. Lynn, Nucl. Phys. **17**, 586 (1960)
- [4] G. E. Brown, Nucl. Phys. **57**, 339 (1964)
- [5] C. F. Clement *et al.*, Nucl. Phys. **66**, 273 (1965); **66**, 293 (1965)
- [6] F. S. Dietrich *et al.*, Phys. Rev. Lett. **38**, 156 (1977)
- [7] S. Raman *et al.*, Phys. Rev. C **32**, 18 (1985)
- [8] H. Feshbach *et al.*, Ann. of Phys. **41**, 230 (1967)
- [9] H. Ikegami, and G. Emery, Phys. Rev. Lett. **13**, 26 (1964)
- [10] N. Michel *et al.*, Phys. Rev. C **67**, 054311 (2003)
- [11] A. J. Koning, and J. P. Delaroche, Nucl. Phys. **A713**, 231 (2003)
- [12] K. Bear, and P. E. Hodgson, J. Phys. G.: Nucl. Phys. **4**, L287, 1978
- [13] S. F. Mughabghab *et al.*, Neutron Cross Sections, Academic Press, NY (1984)
- [14] S. Raman *et al.*, Phys. Rev. C **46**, 972 (1992)
- [15] S. Raman *et al.*, Phys. Rev. C **53**, 616 (1996)
- [16] I. Thompson, private communication.
- [17] K. Grun, and H. Oberhummer, computer code TEDCA, TU Wien, 1995 (unpublished)
- [18] H. Derrien *et al.*, ORNL/TM-2001/271, (2002)
- [19] R. Sayer *et al.*, ORNL/TM-2003/50, (2003)
- [20] I.J. Thompson, Comp. Phys. Rep. **7**, 167 (1988)